Environmental Performance of 3D-Printing Polymerisable Ionic Liquids

Vinícius Gonçalves Maciel,[1,2] Dominic J. Wales,[3,4,†] Marcus Seferin,[1,2] Victor Sans*[3,4]

[1]School of Chemistry, Pontifical Catholic University of Rio Grande do Sul – PUCRS, Brazil
[2]Post-Graduation Program in Materials Engineering and Technology, Pontifical Catholic University of Rio Grande do Sul – PUCRS, Brazil
[3]Faculty of Engineering, University of Nottingham, Nottingham, NG7 2RD, U.K.
[4]GSK Carbon Neutral Laboratory, University of Nottingham, Nottingham, NG7 2GA, U.K.
* victor.sanssangorrin@nottingham.ac.uk

Abstract: This work presents a "cradle-to-gate" Life Cycle Assessment (LCA) of 3D-printing polymerisable ionic liquids (PILs) using digital light projection (DLP). It is based on primary data from environmental emissions, wastewater, chemical components, and manufacturing of PIL based devices. The results indicate that the printing process does not significantly exacerbate the environmental impacts. However, it is shown that excellent opportunities for further mitigation of the life cycle impacts of PILs can be realised are by practising reagent recovery, which reduces the amount of reagents emitted as waste, and by reduction/recycling of solvents used for cleaning the 3D part. The major impact contributor in the 3D-printing of PILs is the synthesis of the IL monomers. The effective reduction of solvent consumption and recovery significantly improves the impact of the synthetic process. This work focuses on the employment of the 3-butyl-1-vinylimidazolium [BVim] cation, with the non-coordinating and hydrophobic bis(trifluoromethane)sulfonimide $[NTf_2]^-$ anion as the counter anion. The polymerisable monomer IL has comparable impact compared to the analogous non-polymerisable 3-butyl-1-methylimidazolium $[NTf_2]^-$ ionic liquid, thus potentially allowing for the more efficient use of the ionic liquid properties by immobilization in solid phases. Furthermore, it is demonstrated that switching the anion from $[NTf_2]^-$ to dicyanamide $[N(CN_2)]^-$ significantly decreases the impacts in all categories evaluated for PIL production. This work represents the first phase toward quantitative LCA data generation for the process of 3D-printing ionic liquids, which will be great support for decision making during design of PIL 3D-printing processes at a laboratory scale.

Key words: Life Cycle Assessment, 3D-printing, additive manufacturing, ionic liquids, stereolithography, polymers

---

[†] Current address: The Hamlyn Centre, Faculty of Engineering, South Kensington Campus, Imperial College London, London, SW7 2AZ, U.K.

1 Introduction

Polymerisable ionic liquids or poly(ionic liquid)s (PILs) (Mecerreyes, 2011) (Yuan et al., 2013) are a type of polyelectrolytes with similar structure to homogeneous ionic liquids (ILs),(Welton, 1999) with an effective transfer of IL properties to the supported phases,(Sans et al., 2011) and are increasingly gaining popularity in a broad range of fields, including energy, catalysis and semiconductors (Yu et al., 2015) (Qian et al., 2017). Despite having been long considered green solvents due to their negligible vapour pressure at STP conditions, life cycle assessment (LCA) of ILs have been performed,(Cuéllar-Franca et al., 2016) and it has been found that employing ILs as solvent is highly likely to have a larger life cycle environmental impact than conventional solvents. (Zhang et al., 2008) Hence, the reduction in gaseous emissions related to the negligible vapour pressure, do not necessarily translate into more sustainable processes (Kralisch et al., 2005). Employing ILs as proxy, it has been found that recovery of the IL and solvents employed are key parameters to optimise the environmental impacts of the modelled processes (Amado Alviz and Alvarez, 2017; Righi et al., 2011; Zhang et al., 2008). Hence, immobilization of the IL should help to mitigate the environmental impacts of processes that employ ILs. Indeed, the effective transfer of properties from the bulk ionic liquids to supported materials with analogous units helps to overcome the limitations typically associated with the employment of ionic liquids, by minimizing the amount of IL units used and facilitating the separation and recycling of the material (Sans et al., 2011).

Additive manufacturing, commonly known as three-dimensional printing (3DP) is a relatively novel manufacturing technology that allow for the generation of complex geometries in a layer by layer fashion (Gunasekera et al., 2016). The additive nature of these techniques minimizes the amount of material employed, potentially lowering energy use, resource demands and related carbon dioxide (CO_2) emissions over the entire product life cycle. It is estimated that the implementation of 3D-printing might allow reduction of energy and carbon dioxide emission intensities by about 5 % by 2025 (Gebler et al., 2014). Furthermore, it may induce changes in manufacturing logistic supply chains, generating shifts towards digital distributed supply chains (Gebler et al., 2014) (OECD, 2017).

However, concerns with 3D-printing have been highlighted by various recent studies in terms of environmental protection and sustainability (Bekker and Verlinden, 2018; Li et al., 2017; Ma et al., 2018a). According to Ma *et al.* (2018) additive manufacture stage has the highest influence on environmental performance. Several studies have reported that many 3D-printing processes have relatively high levels of energy consuption (Barros *et al.*, 2017; Kreiger and Pearce, 2013; Yang et al., 2017). An extensive review of 3D-printing and its societal impact can be found in Huang *et al.* (2013).

Despite the efforts to develop novel materials for 3D-printing, the molecular functionalization of printable 'inks' remains challenging, thus hindering the range of applications accessible with these techniques. Long and collaborators recently demonstrated the possibility of 3D-printing PILs (Schultz *et al*., 2014). Very recently, we demonstrated the possibility of inkjet printing PILs (Karjalainen *et al.*, 2018) and also 3D-printing of advanced photochromic materials based on PILs containing molecular hybrid organic-inorganic polyoxometalates (Wales *et al.*, 2018). Furthermore, the possibility of 3D-printing layers with high resolution (5 μm) employing inkjet allows further minimization of the material employed (Karjalainen *et al.*, 2018).

Despite the potential of these new materials to develop novel applications, there are no specific studies of the environmental impact associated with their manufacture. Understanding the environmental impact of manufacturing PILs is key to enable sustainability based decision-making processes for the development of novel materials, devices and applications using additive manufacture (Cerdas *et al.*, 2017). Life cycle assessment (LCA) is a powerful tool to evaluate the environmental impacts of the product and process involving additive manufacture of PILs (Jacquemin *et al.*, 2012). Here, we present the first cradle-to-gate LCA analysis of the manufacturing of imidazolium-based polymerisable ionic liquids with 3D-printing, with a modular analysis that allows for the identification of the magnitude of the contribution from the different process steps. Primary laboratory scale data was used to model the synthesis of the PIL precursors and the subsequent printing step. Sensitivity analyses were also performed to elucidate how optimisation of the additive manufacture of advanced devices based on PILs can lead to significant reductions in the environmental impacts.

2 Methodology

2.1 Goal and Scope

The goal of this study is to provide a cradle-to-gate LCA analysis of the manufacturing of imidazolium-based PILs with 3D-printing, with a modular analysis that allows for the identification of the magnitude of the contribution from the different process steps. Also, this study aims to understand how these impacts compare to an analogous non-polymerisable homogeneous ionic liquid, and from PIL precursors with a different anion. The synthesis of the ionic liquids and the 3D-printing of the PILs was conducted at laboratory scale. Therefore, these data are considered as primary data. Use of secondary data was necessary to provide intermediate substances and for making comparative scenarios.

The Functional Unit (FU) for this study is a 1.2 g printed part of PIL; all the inputs and outputs are related to the FU. In the "cradle-to-gate" model used in this study, all of the process steps from raw material extraction (the cradle), up to the printed material step (the gate of the laboratory), are considered. The synthesis of poly(ionic liquids) was based on the reported synthesis procedure for 3-butyl-1-vinylimidazolium bis(trifluoromethane)sulfonimide ([BVim][NTf_2]) (Wales *et al.*, 2018). The production of [BVim][NTf_2]) is achieved via a metathesis reaction between lithium bis(trifluoromethane)sulfonimide ($LiNTf_2$) and 3-butyl-1-vinylimidazolium bromide ([BVim][Br]). The system boundaries assessed in this work are defined in **Figure 1**. The LCA study has been performed based on Standards ISO 14040 (ISO, 2006a) and ISO 14044 (ISO, 2006b). Data necessary to model the upstream processes was obtained from the Ecoinvent v3.2 database and Simapro Software v 8.003 version faculty was used for process modelling and impact characterisation.

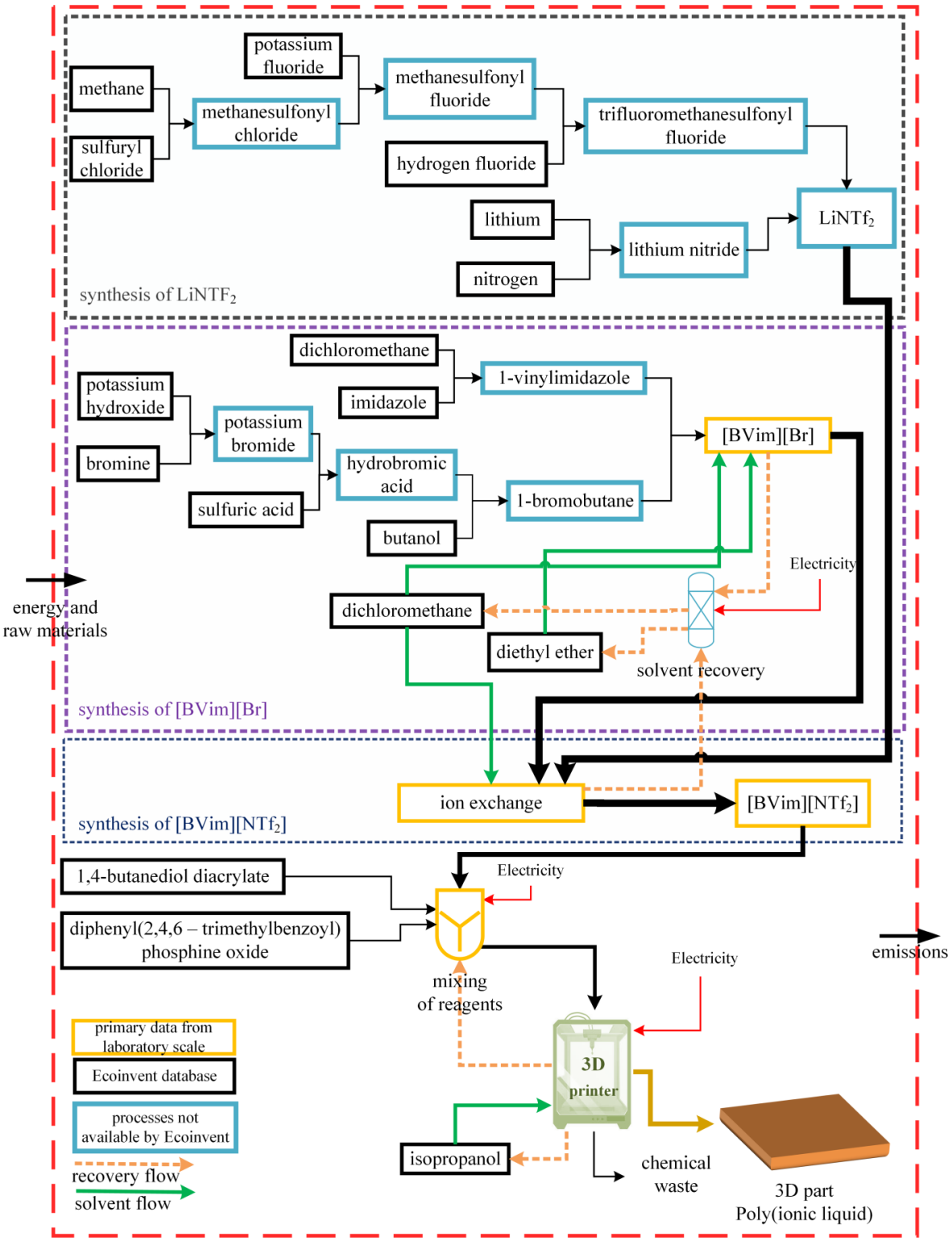

Figure 1. Diagram highlighting the system boundaries of the life cycle assessment presented in this work. [BVim][Br]: 3-butyl-1-vinylimidazolium bromide; [BVim][NTf_2]: 3-butyl-1-vinylimidazolium bis(trifluoromethane)sulfonimide; $LiNTf_2$: lithium bis(trifluoromethane)sulfonimide; IUPAC name for "isopropanol": propan-2-ol.

2.2 Life Cycle Inventory Data Collection

The life cycle material and energy consumption data related to production of the PILs, ILs and their precursors were derived from a combination of mass and energy balance primary data from the laboratory, literature, theoretical calculations, and secondary data sources, such as databases. Full life cycle assessments involving ILs are difficult,(Cuéllar-Franca et al., 2016; Mehrkesh and Karunanithi, 2016, 2013) due to the lack of LCI data for most novel ILs in the literature, because of complex synthetic routes involving numerous precursors. In this work a full life cycle assessment was conducted using the "life cycle tree" approach reported previously to assess the LCA of ILs (Cuéllar-Franca et al., 2016; Mehrkesh and Karunanithi, 2013; Peterson, 2013; Zhang et al., 2008).

2.2.1 Mass balances

The material inputs and outputs of 3D-printing the imidazolium based PILs were obtained from experimental data (see **Table S8** in the ESI). A schematic overview of the 3D printing process is given in the **Scheme 1** and **Scheme 2** in the ESI. The inputs of the [BVim][Br] and [BVim][NTf_2] were collected from primary data generated in the laboratory. The outputs of these substances were calculated from the mass balance (**Tables S1 – S8** in the ESI). The mass balances for PIL precursors that were not available in the Ecoinvent v3.2 database were calculated following literature methods (Felder and Rousseau, 2005). **Table 1** summarises the synthetic routes considered in this study for all substances not available in LCI databases.

Table 1. Synthesis routes considered to chemical substances not available in LCI databases.

Entry	Substance	Abbreviation	Chemical routes assumed	Reference
1	3-butyl-1-vinylimidazolium bromide ($C_9H_{15}BrN_2$)	[BVim][Br]	$C_5H_6N_2 + C_4H_9Br \rightarrow C_9H_{15}BrN_2$	This work
2	1-vinylimidazole ($C_5H_6N_2$)	-	$C_3H_4N_2 + C_2H_4Cl_2 \rightarrow C_5H_6N_2 + 2HCl$	(Ding and Shen, 2012)
3	1-bromobutane (C_4H_9Br)	-	$C_4H_{10}O + HBr \rightarrow C_4H_9Br + H_2O$	(Kamm and Marvel, 1921)
4	hydrobromic acid (HBr)	-	$H_2SO_4 + KBr \rightarrow KHSO_4 + HBr$	(Booth, 1939)
5	potassium bromide (KBr)	-	$6KOH + 3Br_2 \rightarrow KBrO_3 + 5KBr + 3H_2O$	(Blanchard et al., 1936)
6	3-butyl-1-vinylimidazolium bis(trifluoromethane)sulfonimide ($C_{11}H_{15}F_6N_3O_4S_2$)	[BVim][NTf_2]	$C_9H_{15}BrN_2 + C_2F_6LiO_4S_2N \rightarrow C_{11}H_{15}F_6N_3O_4S_2 + LiBr$	This work
7	lithium bis(trifluoromethane)sulfonimide ($C_2F_6LiO_4S_2N$)	$LiNTf_2$	$2CF_3SO_2F + Li_3N \rightarrow C_2F_6LiO_4S_2N + 2LiF$	(Peterson, 2013)
8	lithium nitride (Li_3N)	-	$6Li + N_2 \rightarrow 2Li_3N$	(Peterson, 2013)
9	trifluoromethanesulfonyl fluoride (CF_3SO_2F)	-	$CH_3SO_2F + 3HF \rightarrow CF_3SO_2F + 3H_2$	(Peterson, 2013)
10	methanesulfonyl fluoride (CH_3SO_2F)	-	$CH_3SO_2Cl + KF \rightarrow CH_3SO_2F + KCl$	(Peterson, 2013)
11	methanesufonyl chloride (CH_3SO_2Cl)	-	$CH_4 + SO_2Cl_2 \rightarrow CH_3SO_2Cl + HCl$	(Peterson, 2013)
12	sulfuryl chloride (SO_2Cl_2)	-	$SO_2 + Cl_2 \rightarrow SO_2Cl_2$	(Peterson, 2013)

2.2.2 Energy balances

The energy flow of the 3D-printing process was determined by measuring the energy consumption of the printing process through use of an electricity monitor socket (Brennenstuhl® PM 231E model). This approach has been previously used in lifecycle assessment studies of fabrication at the laboratory scale (Kralisch *et al.*, 2007). Reaction enthalpies were calculated for the different transformations summarised in **Table 1**, except for $LiNTf_2$ which has been previously determined (Peterson, 2013). The theoretical energy consumption for the production of substances was calculated through the use of **Eqs 1-3**. The calculation of the theoretical energy consumption was based on multiplying the reaction enthalpies by a series of correction factors, following literature methods (Cuéllar-Franca *et al.*, 2016; Mehrkesh and Karunanithi, 2013). According to Mehrkesh and Karunanithi,(2013) the estimated theoretical value can be converted to the actual heat consumption (with heating assumed to be supplied by combustion of natural gas) using a correction factor of 4.2 for endothermic and 3.2 for exothermic reactions. It is important to highlight that, in the method by Mehrkesh and Karunanithi, and in this work, an assumption was

made that no work is performed and that the kinetic and potential energy are zero. Thermophysical property data have been extracted from National Institute of Standards and Technology (NIST, 2017) and Society for Chemical Engineering and Biotechnology (DETHERM, 2017) databases. Values for the heat of formation of ionic liquids that were not available in the literature, were calculated (**Table S1**) using a genetic algorithm-based multivariate linear regression method (Vatani *et al.,* 2007). Heat capacities of ionic liquids that were not available in the literature were calculated according to the Joback group contribution method (Stouffer *et al.*, 2008). Sensitivity analysis was performed to estimate the effect of the assumed thermodynamic parameters.

$$E_i = \Delta H \times Fc \qquad \textbf{Eq. 1}$$

$$\Delta H = \sum(RMM.\widehat{H})outputs - \sum(RMM.\widehat{H})inputs \qquad \textbf{Eq. 2}$$

$$\widehat{H} = \Delta\widehat{H}f° + \int_{T1}^{T2} C_R.\Delta T \qquad \textbf{Eq. 3}$$

where:

E_i: theoretical energy consumption

ΔH: heat of reaction

RMM = molecular weight of reactants

$\widehat{H}$= specific enthalpy of reactants

$\Delta\widehat{Hf^\circ}$ = heat of formation of reactants

C_R = calorific value of reactants

T1 = reference temperature (25 ºC)

T2 = temperature of the reactants

Fc= a factor of 4.2 for endothermic reactions with the assumption of natural gas powered heating and a factor of 3.2 for exothermic reactions with the assumption that cooling uses electricity (Mehrkesh and Karunanithi, 2013).

2.3 Life Cycle Impact Assessment and Interpretation

The choice of environmental impact categories is a very important part of an LCA study and impacts categories that permit an overall assessment of impacts must be considered (de Bruijn *et*

al., 2002). Thus, the methods for calculating environmental impacts chosen for this study were CML baseline (PRé Consultants, 2014) and Cumulative Energy Demanded (CED v1.09), which are the most widely employed for life cycle studies on ILs or 3D-printing (Cuéllar-Franca et al., 2016; Huebschmann et al., 2011; Kreiger and Pearce, 2013; Ma et al., 2018b; Righi et al., 2011). The following impact category groups were analysed: global warming potential (GWP), abiotic depletion potentials (ABP), acidification potential (AP), eutrophication potential (EP), human toxicity potential (HTP), ozone layer depletion potential (ODP), fresh aquatic ecotoxicity potentials (FAEP), marine aquatic ecotoxicity potentials (MAEP) and cumulative energy demand (CED). These impact categories were chosen as they have been previously employed in LCA studies of ILs (Amado Alviz and Alvarez, 2017; Cuéllar-Franca *et al.,* 2016; Farahipour and Karunanithi, 2014; Huebschmann *et al.*, 2011; Kralisch *et al.*, 2007, 2005; Mehrkesh and Karunanithi, 2013; Righi *et al.*, 2011; Zhang *et al.*, 2008). Moreover, CED has been reported as an important indicator of sustainability in additive manufacturing (Kellens *et al.*, 2017; Kreiger and Pearce, 2013; Quinlan *et al.*, 2017).

2.4 Assumptions and limitations

For the evaluation of the system, the following assumptions have been made:

Theoretical energy: only the energy requirements of reactors (heating and cooling) have been considered as it is not known what other unit operations may be needed in a future commercial production process and what their configuration and capacity might be. Therefore, energy consumption for separation, pumping and other operations is excluded from the estimation.

Power grid UK: For database consistency, all the laboratorial scale processes analysed in this work were located in United Kingdom (UK). Thus the UK power generation mix (Energy UK, 2017) was considered in this work for the production of [BVim][NTf_2], [BVim][Br] and the 3D-printing step.

Upstream process: For database consistency with the Ecoinvent database 3.2,(Frischknecht et al., 2005) all the industrial processes analysed in this paper were located in Europe. Ecoinvent database establishes transport distances and infrastructure for each process. For potassium fluoride the "Sodium fluoride {GLO}| market for | Alloc Def, U" database within the Ecoinvent v3.2 database was used.

Transport: For those processes not included in the Ecoinvent v3.2 database, the transport of substances was considered as 100 km by lorry and 600 km by train transport within Europe (Hischier et al., 2005).

Emissions of ionic liquids and $LiNTf_2$*:* [BVim][NTf_2], [BVim][Br] and $LiNTf_2$ outputs were considered as unspecified organic compounds in the Simapro software. In this case emissions are defined as all releases of chemicals during the synthesis of the ionic liquids and the utilisation of the ionic liquids.

Solvent recycling: In this study the recycling and refeeding of 99 % of all solvents used for syntheses of [BVim][NTf_2], [BVim][Br] and work-up were assumed (Cuéllar-Franca *et al.*, 2016; Kralisch *et al.*, 2007, 2005). Thus, the impact of recycling the organic solvents isopropanol, diethyl ether and dichloromethane was estimated by assuming the solvent distillation and the energy consumption from thermodynamic data. The energy demand for solvent recycling were calculated using **Eq. 4** according to the work of Felder and Rousseau (2005), with an additional correction factor of either 4.2 or 3.2 (Mehrkesh and Karunanithi, 2013). The results are shown in the Error! Reference source not found..

$$Q_{cal} = (n \times \int_{T1}^{T_{evap}} Cp \times dT + \Delta H_{vap}) \times Fc \qquad \textbf{Eq. 4}$$

Where,

Q_{cal}: Heat transported

n: number of mols

T1 = reference temperature (25 ºC)

T_{evap} = evaporation temperature of the substance

Cp: heat capacity

dT: temperature differential

ΔH_{vap}: Heat of vaporisation

F_C: The estimated theoretical value could be converted to the actual heat consumption (assumed to be supplied by natural gas) using a correction factor of 4.2 and the theoretical energy by exothermic reactions to the actual cooling electricity requirements using a correction factor of 3.2 (Mehrkesh and Karunanithi, 2013).

Table 2. Solvent recycling and theoretical energy calculated by heat transport referenced to the FU.

Entry	Solvent	Process	Amount / mol	ΔH_{vap} / kJ mol^{-1}	$C_p(l)$ / kJ mol^{-1} K^{-1}	Q_{cal} / kJ
1	isopropanol	Washing 3D part	0.11	39.95	0.16	22.40
2	dichloromethane	[BVim][NTf_2]	3.09	28.06	0.10	137.23
3	diethyl ether	[BVim][Br]	0.67	27.10	0.17	118.65
4	dichloromethane	[BVim][Br]	0.16	28.06	0.10	118.52

Overall limitations: In this study, the potential limitations are as follows: (i) all calculations were based on the life-cycle tree and it is possible that alternative methods (reactions) exist for producing one or more of the precursors; (ii) the reaction yields of ionic liquid syntheses were based on the literature when available, and a yield of 100% was assumed when the data was not available; (iii) the calculations in this study are based on small-scale batch processes in laboratory scale experiments for producing the PIL and the ionic liquids ([BVim][NTf_2] and [BVim][Br]).

3 Results and Discussion

3.1 Life Cycle Inventory Results

The LCI results from this work are presented in **Table S8-S10** of the Electronic Supplementary Material. The input and output flows for each substance consider the amounts required to produce one part of PIL (the FU) with a mass of 1.2 g. **Table S8** shows the LCI results from primary data collected at laboratory scale. **Table S9** shows the LCIs of chemical substances that were employed in the synthesis of [BVim][Br] and were not available in the Ecoinvent v3.2 database. **Table S10** shows the LCIs of $LiNTf_2$ and its intermediate chemical substances.

3.2 Life cycle Assessment Results

Once all input and output flows and their amounts had been determined, the next step was to determine the impacts attributed to manufacturing one of the FU. Thus, the environmental impacts for each environmental impact category caused by the production of the FU are shown in **Table 3**.

Table 3. Characterised LCA results of one 3D printed part (1x FU).

Entry	Impact Categories	Unit	PIL printed	Method
1	Abiotic depletion	kg Sb eq.	7.87×10^{-4}	CML 2001
2	Acidification	kg SO_2 eq.	3.14×10^{-3}	CML 2001
3	Cumulative Energy Demand	MJ	1.74	CED
4	Eutrophication	kg PO_4^{3-} eq.	5.33×10^{-5}	CML 2001
5	Freshwater aquatic ecotoxicity	kg 1,4-DB eq.	1.21×10^{-3}	CML 2001
6	Global warming	kg CO_2 eq.	9.19×10^{-2}	CML 2001
7	Human toxicity	kg 1,4-DB eq.	6.46×10^{-2}	CML 2001
8	Marine aquatic ecotoxicity	kg 1,4-DB eq.	7.50×10^{-3}	CML 2001
9	Ozone layer depletion	kg CFC-11 eq.	1.85×10^{-8}	CML 2001

CML 2001: CML method 2001. (PRé Consultants, 2014) CED: Cumulative Energy Demand V1.09 method.(PRé Consultants, 2014) FU: functional unit used in this work = 1.2 g of PIL printed. Sb = antimony, SO_2 = sulfur dioxide, PO_4^{3-} = phosphate, CO_2 = carbon dioxide, CFC-11 = trichlorofluoromethane, 1,4-DB = 1,4-dichlorobenzene, MJ = mega joules.

Due to a lack of life cycle studies on 3D-printing of polymerisable ionic liquids, studies about 3D-printing manufacture of non-ionic liquid polymers were employed for comparison *(Cerdas et al.*, 2017). Regarding the global warming potential, the impact magnitude was 9.19×10^{-2} kg CO_2 eq. / 1.2 g of PIL printed. In comparison, Cerdas *et al.*(2017) reported a LCA study of 3D-printing products from polylactic acid employing Fused Deposition Modelling (FDM) and stated that the production of one frame for eyeglasses (~30 g) gave rise to a GWP impact of between 0.006-0.021 kg CO_2 eq. / g of part. This means that even though both processes are not directly comparable, the PILs have higher GWP (0.0785 kg CO_2 eq. / g of PIL printed).

In order to determine the contribution of inputs in the 3D-printing step (reagents, solvents, heat and electricity consumed) on the life cycle of the PIL, a contribution analysis of this step was made (see **Figure 2**). The results indicate that the ionic liquid [BVim][NTf_2] was the major source of impacts for all environmental categories evaluated. In contrast, the additive manufacturing step (3D-printing process) did not show a significant contribution to the final results. Also, the electricity energy consumed for 3D-printing had an impact contribution between 0.86 % and 6.9 %. Energy consumption of 3D manufacturing processes is an important environmental performance consideration for additive manufacturing (Gebler *et al*., 2014; Gutowski *et al*., 2017; Peng, 2016). In this study the energy consumed during printing was 8.91 kWh/kg of PIL printed

by stereolithography (SLA). This result is in agreement with previous reports, which found that the energy consumption of various additive manufacture technologies ranges between 1.11 kWh/kg to 2140 kWh/kg (Gutowski *et al.*, 2017). Another previous study reported the energy consumed during a stereolithography manufacture process using epoxy resin was 32.5 kWh/kg (Yanchun Luo *et al.*, 1999). Yang *et al.* (2017) developed a mathematical model for the energy consumption of SLA-based processes where according to their results the layer and total printing time are major factors significant to the overall energy consumed. In addition, Yang *et al.* calculated using their mathematical model that the energy consumed to print LS600M material (a commercial photopolymer) is 175.95 kWh/kg of material printed (Yang et al., 2017).

The energy consumed at laboratory scale for mixing and preparation of reagents plus the electrical energy consumed during 3D-printing had a contribution of 1.60 % and 13.3 % for ozone layer depletion and global warming, respectively. The mixing and preparation of reagents steps can be considered independent of the use of the 3D printer, since these steps are necessary in traditional synthesis (Shaplov et al., 2016).

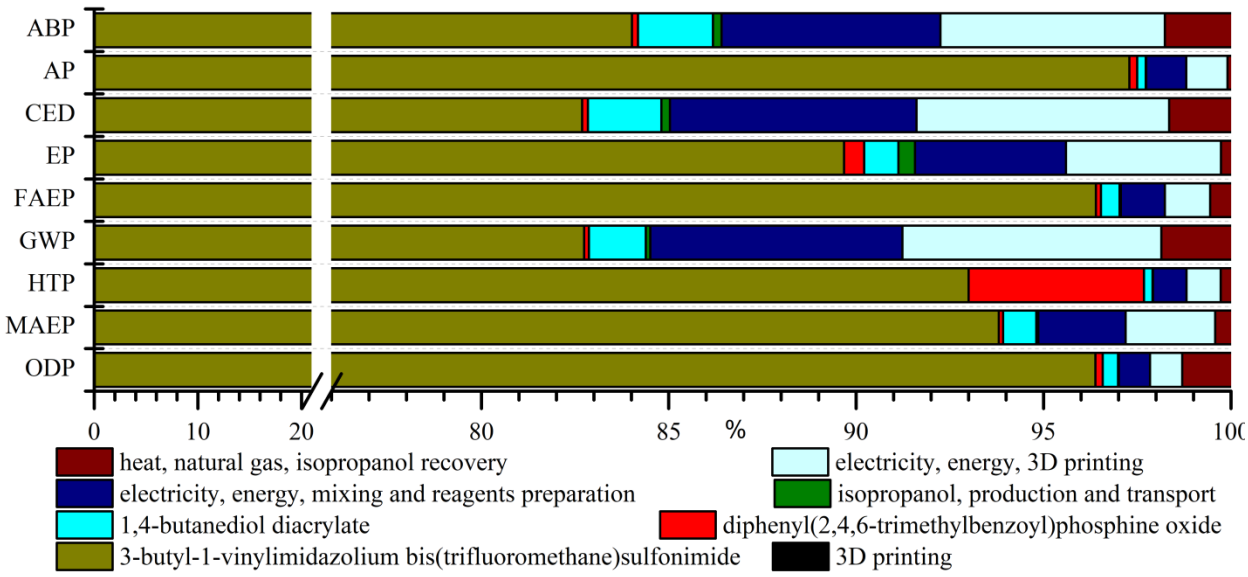

Figure 2. Contribution relative of inputs to life cycle of PIL printed

The [BVim][NTf_2] synthesis process presents a long supply chain from natural resources to the end product, therefore it requires large quantities of materials, energy and solvents, and it involves organic compound emissions to air and water. The total score of each environmental impact category resulting from classification and characterization of the compounds used in the synthesis of [BVim][NTf_2] production are shown in Error! Reference source not found.. Previous studies reported the environmental performance of other ionic liquids such as butylmethylimidazoluim

chloride [Bmim][Cl], (Amado Alviz and Alvarez, 2017; Righi *et al.*, 2011) and trihexyltetradecylphosphonium 1,2,4-triazolide ([P_{66614}][124Triz]) (Cuéllar-Franca *et al.*, 2016). These studies reported GWP impacts estimated at 6.30 kg CO_2 eq. per kg of [P_{66614}][124Triz] and 6.40 kg CO_2 per kg [Bmim][Cl]. In this work, the [BVim][Br] showed similar environmental performance (8.9 kg CO_2/kg of [BVim][Br]), however the $LiNTf_2$ and [BVim][NTf_2] showed higher emissions. Huebschmann *et al.*(2011) reported large differences between environmental performances of ionic liquids using life cycle methodology. In that study, the [Bmim][Cl] showed GWP impacts five times smaller than 1-octadecyl-3-methylimidazolium bromide ([C_{18}MIM][Br]) (Huebschmann et al., 2011).

Table 4. Cradle-to-gate life cycle assessment results for production of 1 kg of the ionic liquids and $LiNTf_2$ used in this study.

Entry	Impact categories	Unit	[BVim][Br]	$LiNTf_2$	[BVim][NTf_2]	Method
1	Abiotic depletion	kg Sb eq.	8.89×10^{-2}	1.46×10^{-1}	2.17×10^{-1}	CML 2001
2	Acidification	kg SO_2 eq.	7.26×10^{-1}	5.22×10^{-1}	1.00	CML 2001
3	Cumulative Energy Demand	MJ	183	323	475	CED
4	Eutrophication	kg PO_4^{3-} eq.	5.45×10^{-2}	1.08×10^{-2}	1.57×10^{-2}	CML 2001
5	Freshwater aquatic ecotoxicity	kg 1,4-DB eq.	3.78×10^{-1}	1.43	3.83×10^{-1}	CML 2001
6	Global warming	kg CO_2 eq.	8.98	17.1	25.0	CML 2001
7	Human toxicity	kg 1,4-DB eq.	28.2	2.77	19.8	CML 2001
8	Marine aquatic ecotoxicity	kg 1,4-DB eq.	9.25×10^{-1}	15.6	2.31	CML 2001
9	Ozone layer depletion	kg CFC-11 eq.	1.62×10^{-6}	4.42×10^{-6}	5.87×10^{-6}	CML 2001

[BVim][Br]: 3-butyl-1-vinylimidazolium bromide; $LiNTf_2$: Lithium bis(trifluoromethane)sulfonimide; [BVim][NTf_2]: 3-butyl-1-vinylimidazolium bis(trifluoromethane)sulfonimide; CED: Cumulative Energy Demand V1.09. Sb = antimony, SO_2 = sulfur dioxide, PO_4^{3-} = phosphate, CO_2 = carbon dioxide, CFC-11 = trichlorofluoromethane, 1,4-DB = 1,4-dichlorobenzene, MJ = mega joules.

Figure 3 shows the relative impact contribution of the three steps of the [BVim][NTf_2] synthesis: (Step 1) synthesis of $LiNTf_2$; (Step 2) synthesis of 3-butyl-1-vinylimidazolium bromide and (Step 3) the synthesis of [BVimi][NTf_2]. The results suggest that $LiNTf_2$ is the biggest contributor to the environmental impacts in the [BVim][NTf_2] life cycle. On the other hand, Step 3 shows the lowest contribution. The $LiNTf_2$ represents 65.2 % of total mass of the reagents consumed in the synthesis of [BVim][NTf_2], and 39.4 % is considered to be chemical waste output. Hence, good practices

related to this reaction are necessary to obtain a good environmental performance of the [BVim][NTf_2] product. An environmental improvement for [BVim][NTf_2], and consequently the imidazolium-based PIL, could be achieved by development of new synthesis routes or synthesis routes that require less $LiNTf_2$ input.

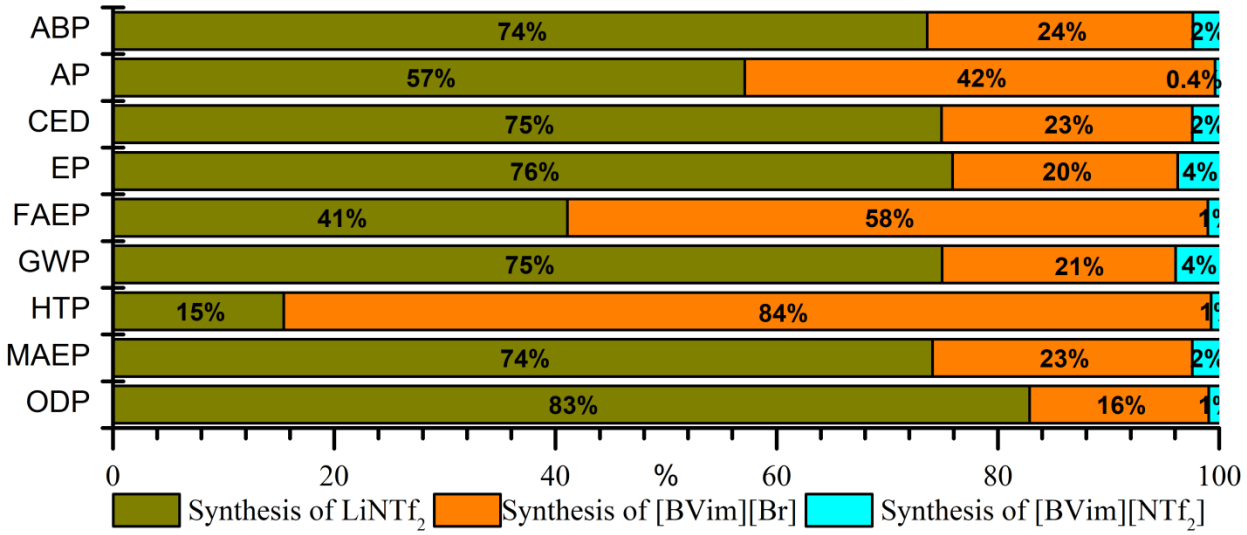

Figure 3. Life cycle Assessment results of [BVim][NTf_2] step syntheses for impact categories. GWP: global warming potential; ABP: abiotic depletion potentials; AP: acidification potential; EP: eutrophication potential; HTP: human toxicity potential: ODP: ozone layer depletion potential; FAEP: fresh aquatic ecotoxicity potentials; MAEP: marine aquatic ecotoxicity potentials and CED: cumulative energy demanded.

3.2.1 Contribution of processes

Figure 4 shows the percentage contributions of each impact categories for the main impact processes for printing PILs. Processes that showed a contribution ≥5 % were considered a significant contribution. Contributions of <5 % were added together and named “other processes”.

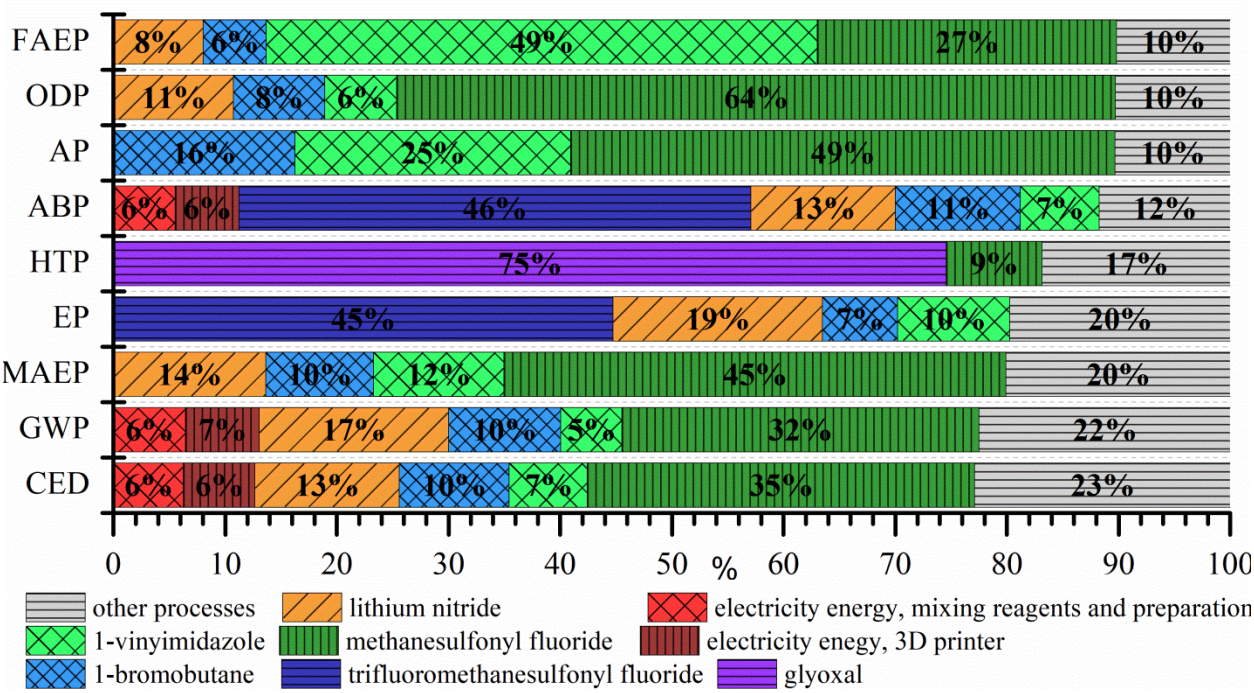

Figure 4. Life cycle processes contribution analysis. GWP: global warming potential; ABP: abiotic depletion potentials; AP: acidification potential; EP: eutrophication potential; HTP: human toxicity potential: ODP: ozone layer depletion potential; FAEP: fresh aquatic ecotoxicity potentials; MAEP: marine aquatic ecotoxicity potentials and CED: cumulative energy demanded.

Based on the contribution analysis (see **Figure 4**), it can be observed that the methanesulfonyl fluoride (CH_3SO_2F) showed a significant contribution in seven of the nine impact categories assessed, and it was the major source of impact in four categories. Methanesulfonyl fluoride (CH_3SO_2F) is a precursor in the synthesis of trifluoromethanesulfonyl fluoride, which in turn is an intermediate in the synthesis of $LiNTF_2$. Thus, these results are consistent with the IL being the largest contributor to the environmental impact in this system. In contrast, the methanesulfonyl fluoride did not show significant contribution to either human toxicity potential or abiotic depletion potential. However, both those impact categories showed a significant contribution of trifluoromethanesulfonyl fluoride which is a substance synthesized from methanesulfonyl fluoride. In the Abiotic Depletion Potential (ABP) category, the trifluoromethanesulfonyl fluoride life cycle contributed the most (46.0 %). This is mostly due to the energy consumed for upstream processes. In terms of the substance, combustion of natural gas was the largest contributor with *ca.* 40 % and combustion of hard coal contributed *ca.* 29 % - both of these substances are used for generation of the thermal energy and electricity energy consumed during the trifluoromethanesulfonyl fluoride life cycle. The Acidification Potential (AP) category has methanesulfonyl fluoride and 1-

vinyimidazole as the biggest contributors with 49.0 % and 25.0 %, respectively. In terms of substances in the synthesis of methanesulfonyl fluoride, sulfuric acid emissions to air and water were the biggest contributor in ACP with 29.0 % participation. Besides that, the sulfur dioxide emitted to air showed contribution about 27.7 % for this category. In the eutrophication potential 45.0 % of impacts was coming from trifluoromethanesulfonyl fluoride and 19.0 % from lithium nitride. In terms of substance, nitrogen oxide showed participation of 47.4 % and phosphate emitted to water has participation of 28.6 % in the life cycle of the PIL. It is important to highlight that these processes are intermediate substances used in the synthesis of $LiNTf_2$.

The FAEP and MAEP impact categories have the similar processes and substances as the biggest contributors. Methanesulfonyl fluoride showed contribution of the 27.0 % and 45.0 % for FAEP and MAEP, respectively. Also, 1-vinyimidazole showed contribution of the 49 % and 12 % for FAEP and MAEP, respectively. Besides that, lithium nitride had the next greatest contribution with about 6 % for FAEP and 10 % for MAEP. Note that methanesulfonyl fluoride and lithium nitride are direct precursors in the synthesis of $LiNTf_2$. Moreover, the substance that contributes most for FAEP was formaldehyde with participation of 42.3 %. In MAEP vanadium was the substance that had the major contribution with 34.9 %. The human toxicity impact category showed great contribution from glyoxal production (75.0 %). Glyoxal is used as an intermediate in the synthesis of imidazole, which in turn is an intermediate substance in the synthesis of 3-butyl-1-vinylimidazolium bromide. Also, the impact is dominated by ethylene oxide emissions (48.8 % for water and 25.4 % for air). This substance has been previously reported in LCA studies as contributing greatly to the environmental performance of substances that have imidazole as a precursor (Amado Alviz and Alvarez, 2017; Righi et al., 2011).

Ozone layer depletion also showed methanesulfonyl fluoride as the biggest source of its impacts with participation of 64 %. The intermediate substances to methanesulfonyl fluoride that contribute the most is tetrachloromethane (CFC-10) with participation of 65.9 %. In the accumulative energy demand methane sulfonyl fluoride and isopropanol were the biggest contributors to this impact category, with participation of 26.0 % and 16.0 %, respectively. In terms of substances, natural gas is the largest contributor with 32.9 %, followed by crude oil, which contributed 25.2 %. Both of these substances are used for generation of the thermal energy and electricity energy consumed

during the methanesulfonyl fluoride process. Natural gas represents *ca.* 41 % of source energy in the United Kingdom power generation mix (Energy UK, 2017).

Finally, global warming potential (GWP) has methanesulfonyl fluoride and lithium nitride as the biggest contributors to this impact category, with participation of 32.0 % and 17.0 %, respectively. In terms of substances the GWP was dominated by fossil fuel CO_2 emissions. Fossil fuel CO_2 emissions account for 89.7 % of total GWP, with methane accounting for 7.40 %. However, it was not possible to identify the greatest source of these emissions in the $LiNTf_2$ life cycle (including the methanesulfonyl fluoride and lithium nitride processes). This can be explained by the large number of processes that each contribute a small proportion to the emissions. Therefore, these results suggest that for a reduction of GWP, reduction of emissions must be focused on the chemical formulation or upstream processes of the IL life cycle. Summarizing, the results of contribution analysis indicate that the intermediate substances of $LiNTf_2$ had the largest contribution of environmental impacts on the life cycle of PIL printed in seven of nine the categories studied. Also, the 3D-printing step did not make a significant contribution to the overall total electrical energy consumed.

3.2.2 Sensitivity Analysis

A sensitivity analysis was performed to assess the robustness of the results and to understand the potential effects of changing the experimental methodology, leading to development of best practises.(Amado Alviz and Alvarez, 2017) In this study the sensitivity analysis was applied to: (i) thermodynamic parameters used for extrapolating theoretical energy calculations; (ii) reagent recovery in the 3D manufacturing step; and (iii) recovery of solvent that was used for syntheses of $[BVim][NTf_2]$, [BVim][Br] and for cleaning the 3D printed part.

3.2.2.1 Effect of thermodynamic parameters calculated

The influence of the heat of formation and heat capacity parameters calculated for substances for which this data was not readily available was studied through a sensitivity analysis. The effect of

using these data has been considered by varying the impacts of these parameters (arbitrarily) by ± 50%. As it is possible to observe in **Table S22**, the results indicate that the LCA results demonstrated low sensitivity to the degree of variation in the thermodynamic parameters that were evaluated in this work.

3.2.2.2 Effect of reagent recovery in the 3D manufacturing step

The influence of the recovery of the reagent mixture after the 3D-printing step on the environmental profile of the life cycle was modelled by comparing four different degrees of recovery. It was determined that the degree of reagent formulation recovery, which was performed in the primary data experimental work for this study, was 73.8%. The *ca.* 25% loss of reagent formulation in this step occurs due to a small amount of print reagent formulation remaining in the processing area of the 3D printer. However, optimization of the process could significantly improve this figure. Thus, the influence of the degree of reagent recovery was studied. Four degrees of reagent formulation recovery were investigated; 73.8%, 80.0%, 90.0% and 100%. **Table 5** shows the effect of each degree of reagent recovery on each environmental impact categories. As expected, the environmental impact scores are reduced as the reagent recovery rate increases. For example, for the global warming impact category the reduction was calculated to be 59.0 % for full recovery (100 % reagent recovery). Also, **Figure 5** shows a relative comparison of the life cycle impacts of PIL production using those recovery rates. These results show that reagent recovery is critical as it can significantly reduce the environmental impacts of the PIL printed. Note that for this analysis the inputs and outputs of 3D-printing step (reagents, waste of reagents and reagent recovery) had been changed for each rate of recovery investigated. Also, the energy consumed for mixing and preparation of reagents was re-calculated considering the input of recovered reagent formulation. The flows assumed for this analysis are in the **Tables S11** and **S12** in the electronic supplementary material.

Table 5. Effect of solvent recovery rate on environmental impact categories producing 1.2 g of PIL printed.

			Reagent recovery rate			
Entry	Impact categories	Unit	73.8 %[a]	80%	90%	100%
1	Abiotic depletion	kg Sb eq.	7.87×10^{-4}	6.76×10^{-4}	4.96×10^{-4}	3.17×10^{-4}
2	Acidification	kg SO_2 eq.	3.14×10^{-3}	2.66×10^{-3}	1.89×10^{-3}	1.13×10^{-3}
3	Cumulative Energy Demand	MJ	1.74	1.50	1.10	7.10×10^{-1}
4	Eutrophication	kg PO_4^{3-} eq.	5.33×10^{-5}	4.55×10^{-5}	3.29×10^{-5}	2.04×10^{-5}

5	Freshwater aquatic ecotoxicity	kg 1,4-DB eq.	1.21×10^{-3}	1.03×10^{-3}	7.33×10^{-4}	4.38×10^{-4}
6	Global warming	kg CO_2 eq.	9.19×10^{-2}	7.09×10^{-2}	5.83×10^{-2}	3.76×10^{-2}
7	Human toxicity	kg 1,4-DB eq.	6.46×10^{-2}	5.48×10^{-2}	3.89×10^{-2}	2.32×10^{-2}
8	Marine aquatic ecotoxicity	kg 1,4-DB eq.	7.50×10^{-3}	6.38×10^{-3}	4.58×10^{-3}	2.77×10^{-3}
9	Ozone layer depletion	kg CFC-11 eq.	1.85×10^{-8}	1.57×10^{-8}	1.13×10^{-8}	6.76×10^{-9}

[a] Reagent recovery rate data from laboratory scale. Sb = antimony, SO_2 = sulfur dioxide, PO_4^{3-} = phosphate, CO_2 = carbon dioxide, CFC-11 = trichlorofluoromethane, 1,4-DB = 1,4-dichlorobenzene, MJ = mega joules.

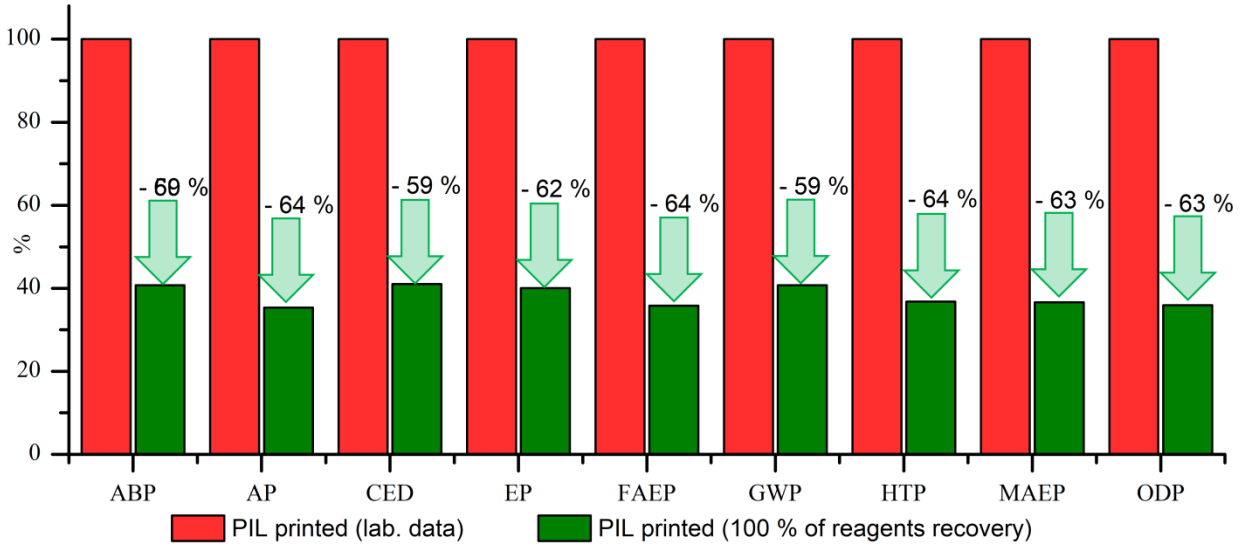

Figure 5. Comparison of the life cycle impacts of PIL with reagent recovery of ~74 % (Lab data) and 100 % in the 3D-printing step.

3.2.2.3 Effect of solvent recovery

Several studies suggest that the solvent recovery is a key parameter in the environmental assessment and an important task for chemical engineers to minimize burden upon the environment (Righi et al., 2011). Thus, in this study, two scenarios for the recovery of organic solvents used in this work were calculated. The first scenario (S1) is the standard scenario of this study where it was considered that there was a recycling and refeeding of 99% of all solvents used for the syntheses of [BVim][NTf_2], [BVim][Br] and used to clean the 3D part. In the second scenario (S2) all organic solvent consumed in these processes were assumed as not recovered. The solvents not recovered were considered as 100 % emitted to air. The results of this analysis are show in **Table 6** and the Error! Reference source not found. shows a LCA results comparison between S1 and S2 for use of the organic solvent. Note that the flows of energy consumed for recycling the solvent

for S2 were changed as well as the amount of waste solvent. These estimations are given in **Table S13** of the electronic supplementary material.

Table 6. Influence of solvent recovery on life cycle impacts of PIL printed (1.2 g of PIL printed).

Impact Categories	Unit	S1 (with solvent recovery)	S2 (without solvent recovery)	Difference
Abiotic depletion	kg Sb eq.	7.87×10^{-4}	1.16×10^{-3}	+ 48 %
Acidification	kg SO_2 eq.	3.14×10^{-3}	3.41×10^{-3}	+ 9 %
Cumulative Energy Demand	MJ	1.74	2.62	+ 50 %
Eutrophication	kg PO_4^{3-} eq.	5.33×10^{-5}	9.86×10^{-5}	+ 85 %
Freshwater aquatic ecotoxicity	kg 1,4-DB eq.	1.21×10^{-3}	1.32×10^{-3}	+ 9 %
Global warming	kg CO_2 eq.	9.19×10^{-2}	2.26×10^{-1}	+ 146 %
Human toxicity	kg 1,4-DB eq.	6.46×10^{-2}	8.40×10^{-2}	+ 30 %
Marine aquatic ecotoxicity	kg 1,4-DB eq.	7.50×10^{-3}	8.58×10^{-3}	+ 14 %
Ozone layer depletion	kg CFC-11 eq.	1.85×10^{-8}	2.10×10^{-8}	+ 14 %

Sb = antimony, SO_2 = sulfur dioxide, PO_4^{3-} = phosphate, CO_2 = carbon dioxide, CFC-11 = trichlorofluoromethane, 1,4-DB = 1,4-dichlorobenzene, MJ = mega joules.

The results indicate that solvent recovery had significant impact for all impact categories that were evaluated. The impact categories abiotic depletion, eutrophication, global warming and cumulative energy demand exhibited the biggest differences between the scenarios S1 and S2, demonstrating that these impact categories were the more sensitive to solvent recycling. Moreover, the recovery of solvent promoted reduction of life cycle impacts of [BVim][NTf_2] in all categories evaluated (S1) (see **Figure S1** in the ESI). Also, the solvents employed for synthesis of ionic liquids were the major contributors to increasing the impacts in S2 (see **Figure S1** and **Table S14** in the ESI). Furthermore, the impact of energy consumed for recovery of the isopropanol, employed for cleaning the 3D part, did not show significant contribution (<1.8 %). These results suggest that emissions of solvent at lab-scale had a big environmental impact and thus good practices for reduction of solvent consumption and increased recovery must be applied. Moreover, solvent recovery is a critical process as it can reduce significantly the environmental impacts of the printed PIL life cycle.

3.3 Comparison between monomer IL and conventional IL

The major impact contributor in the printing of PILs is the synthesis of the IL monomers. For this reason, it is important to understand how these impacts compare to an analogous homogeneous

ionic liquid (*e.g.* **Figure 6**). It is expected that by printing the PIL, the impact of the material during its utilisation phase (cradle-to-grave) will be reduced compared to the homogeneous IL due to simplified protocols for handling and reutilisation of the polymers. Therefore, the conventional IL 3-butyl-1-methylimidazolium bis(trifluoromethane)sulfonimide [Bmim][NTf_2] was chosen as it has a similar structure to 3-butyl-1-vinylimidazolium bis(trifluoromethane)sulfonamide [BVim][NTf_2]. However, [BVim][NTf_2] has additional advantages such as the possibility of being polymerisable (Shaplov et al., 2016); functionalization versatility is afforded by the double bond functional group moiety Therefore, a comparison for production of 1 kg of each ionic liquid was made. The data used for this assessment can be found in **Section 9** of the **ESI**.

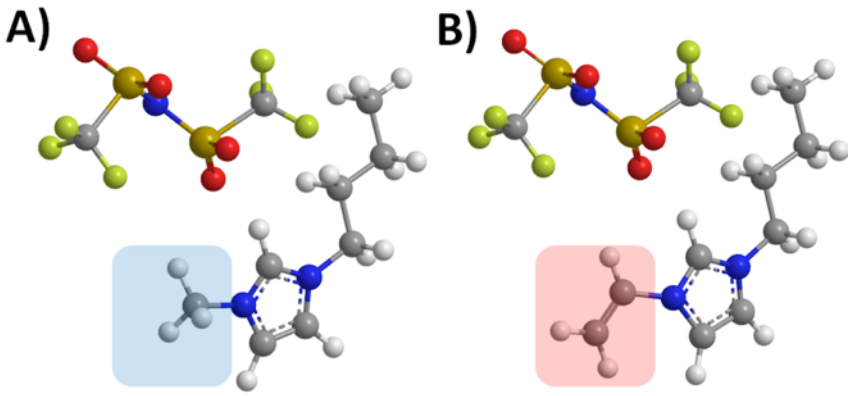

Figure 6. Structures of [Bmim][NTf_2] (A) where the methyl group is shaded light blue and [BVim][NTf_2] (B), where the vinyl group is highlighted in pink.

Table 7. LCA results of production of monomer IL and conventional IL (results for 1 kg of IL)

Entry	Impact categories	Unit	[BVim][NTf_2]	[Bmim][NTf_2]	Difference
1	**Abiotic depletion**	kg Sb eq.	0.22	0.19	- 12%
2	**Acidification**	kg SO_2 eq.	1.01	0.54	- 46%
3	**Cumulative Energy Demand**	MJ	475	428	- 10%
4	**Eutrophication**	kg PO_4^{3-} eq.	1.57×10^{-2}	1.26×10^{-2}	- 20%
5	**Freshwater aquatic ecotoxicity**	kg 1,4-DB eq.	0.38	0.23	- 40%
6	**Global warming**	kg CO_2 eq.	25.00	20.98	- 16%
7	**Human toxicity**	kg 1,4-DB eq.	19.8	47.7	+ 141%
8	**Marine aquatic ecotoxicity**	kg 1,4-DB eq.	2.31	2.03	- 12%
9	**Ozone layer depletion**	kg CFC-11 eq.	5.87×10^{-6}	4.77×10^{-6}	- 19%

Sb = antimony, SO_2 = sulfur dioxide, PO_4^{3-} = phosphate, CO_2 = carbon dioxide, CFC-11 = trichlorofluoromethane, 1,4-DB = 1,4-dichlorobenzene, MJ = mega joules.

The results indicate that the nature of the vinylimidazolium cation of the monomer had comparable impact compared to the non-polymerisable conventional IL. **Figure S4** in the ESI shows a comparison of contribution of the different processes to the life cycle impact categories for [BVim][NTf_2] and [Bmim][NTf_2]. The [BVim][NTf_2] presents less impact for human toxicity than [Bmim][NTf_2] (**Table 7**). In this study, for production of 1kg of the [BVim][NTf_2] 0.239 kg of glyoxal are consumed, compared to 0.669 kg in the synthesis of [Bmim][NTf_2]. Glyoxal is used in the synthesis of imidazole,(Ebel *et al.*, 2002) which in turn is an intermediate substance used in the synthesis of [BVim][Cl] and [Bmim][Cl]. Based on the contribution analysis (see **Figure S4**) it is possible to claim that in general the methanesulfonyl chloride (CH_3ClO_2S) and sodium fluoride showed the most significant contribution in seven of nine impact categories assessed for both IL. Methanesulfonyl chloride and sodium fluoride are used in the synthesis of trifluoromethanesulfonyl fluoride which is an intermediate chemical during synthesis of $LiNTF_2$. Summarizing, the most significant life cycle impacts of monomer and conventional IL that have NTf_2^- in their structure arise due to the anion synthetic process.

3.4 Comparison between the effect of PIL anion on LCA

This study has focussed on the employment of a vinylimidazolium-based cation the $[BVim]^+$ cation with the non-coordinating and hydrophobic $[NTf_2]^-$ as the counter anion,(Karjalainen *et al.*, 2014) leading to stable ILs with low viscosity that are relatively easy to handle and process. Nevertheless, as demonstrated in this work, the largest LCA impact is associated with the synthesis

of the anion. Hence, it is interesting to compare the overall LCA of the use of PIL precursors with a different anion. The large environmental impact associated with the anion synthesis is not surprising due to the large number of synthetic steps required. The $[NTf_2]^-$ was compared to another anion that led to a printable PIL; the dicyanamide anion $[N(CN)_2]^-$. The data used for this assessment can be found in **Section 8** of the ESI. 1.2 g of each compound, and two scenarios of reagent recovery were assumed. Scenario 1 (S1) considered the production of 1.2 g of compound without reagent recovery and the Scenario 2 (S2) considered with full reagent recovery. As is evident in **Table 8**, the change of anion significantly decreased the impacts in all categories evaluated. However, the magnitude of the difference is smaller with full reagent recovery, which is attributed to the difference in mass of the $[N(CN)_2^-]$ and $[NTf_2^-]$ anions.

Table 8. Comparison of the effect of changing the anion for priting 1.2 g of PILs for scenario of reagent recovery

			Anion		
Impact categories	Unit	Scenario	$[NTf_2^-]$	$[N(CN)_2^-]$	Difference
Abiotic depletion	kg Sb eq.	S1	7.87×10^{-4}	4.32×10^{-4}	-45 %
		S2	3.17×10^{-4}	2.55 x 10-4	-20 %
Acidification	kg SO_2 eq.	S1	3.14×10^{-3}	1.57×10^{-3}	-50 %
		S2	1.13×10^{-3}	7.64×10^{-4}	-26 %
Eutrophication	kg PO_4^{3-} eq.	S1	5.33×10^{-5}	2.44×10^{-5}	-54 %
		S2	2.04×10^{-5}	1.39×10^{-5}	-32 %
Global warming	kg CO_2 eq.	S1	9.19×10^{-2}	5.14×10^{-2}	-44 %
		S2	3.76×10^{-2}	3.07×10^{-2}	-18 %
Ozone layer depletion	kg CFC-11 eq.	S1	1.85×10^{-8}	7.36×10^{-9}	-60 %
		S2	6.76×10^{-9}	4.03×10^{-9}	-40 %
Human toxicity	kg 1,4-DB eq.	S1	6.46×10^{-2}	6.33×10^{-2}	-2 %
		S2	2.32×10^{-2}	3.35×10^{-2}	+44 %
Freshwater aquatic ecotoxicity	kg 1,4-DB eq.	S1	1.21×10^{-3}	8.53×10^{-4}	-29 %
		S2	4.38×10^{-4}	4.53×10^{-4}	+4 %
Marine aquatic ecotoxicity	kg 1,4-DB eq.	S1	7.50×10^{-3}	3.21×10^{-3}	-57 %
		S2	2.77×10^{-3}	1.77×10^{-3}	-36 %
Cumulative Energy demand	MJ	S1	1.74	9.47×10^{-1}	-46 %
		S2	7.10×10^{-1}	5.65×10^{-1}	-20 %

S1: No reagent recovery; S2: full reagent recovery. Sb = antimony, SO_2 = sulfur dioxide, PO_4^{3-} = phosphate, CO_2 = carbon dioxide, CFC-11 = trichlorofluoromethane, 1,4-DB = 1,4-dichlorobenzene, GJ = giga joules.

3.5 Conclusions

LCA study for the process of DLP-based 3D-printing of imidazolium-based PILs has been presented. The results indicate that the additive manufacturing process is technically viable and does not exacerbate the environmental impacts from synthesising the constituent monomeric ionic liquids. However, this study also highlights that there are excellent opportunities for mitigating the life cycle impacts of PIL associated with the synthetic steps, mainly through the reduction of reagents emitted as waste by practising reagent recovery and reduction/recycling of solvents used for cleaning the 3D part. This work has focused on the employment of 3D-printing, using digital light projection, of a polymerisable ionic liquid, with the vinylimidazolium-based $[BVim]^+$ cation, and the non-coordinating and hydrophobic $[NTf_2]^-$ as the counter anion. The contribution analysis results suggest that the anion had the largest contribution to the environmental impacts on the life cycle of the PIL studied manly due of intermediate substances (methanesulfonyl fluoride and lithium nitride) used for synthesis of $LiNTf_2$. Overall good practice relating to the synthesis of the [BVim][NTf_2] ionic liquid is necessary to minimise the environmental performance.

A comparison between polymerizable and the analogous homogeneous ionic liquid has been made. The results indicate that the nature of the PIL monomer had comparable impact compared to the structurally similar conventional non-polymerisable IL. This result suggests that PIL monomers are viable in terms of environmental impacts with the additional advantage of versatility due to the double-bond structure.

Comparative analysis of the use of PIL precursors with a different anion indicated that the change of anion has influence on the environmental performance of PILs. The change of anion bis(trifluoromethane)sulfonimide anion $[NTf_2^-]$ to dicyanamide anion $[N(CN)_2^-]$ significantly decreased the impacts in all categories evaluated for PIL production. However, the magnitude of the difference is smaller with full reagent recovery. This suggests that full reagent recovery is just as crucial as the choice of anion in terms of environmental performance of 3D-printing of PIL.

This works represents the first LCA study, which will be of great support for decision making for PIL 3D-printing processes at a laboratory scale. The results of this study help to identify the main aspects and environmental impacts involving the production of the monomer ILs, PILs and the additive manufacturing.

Acknowledgments

V.G-M. and M.S. wish to thank the Brazilian Government by National Council for the Improvement of Higher Education (*CAPES*) support. The University of Nottingham is gratefully acknowledged for the Research Priority Areas for funding.

List of symbols (alphabetical):

Cp: heat capacity

C_R = calorific value of reactants

dT: temperature differential

E_i: theoretical energy consumption

Fc= a factor of 4.2 for endothermic reactions with the assumption of natural gas powered heating and a factor of 3.2 for exothermic reactions with the assumption that cooling uses electricity

ΔH: heat of reaction

$\widehat{H}$= specific enthalpy of reactants

$\Delta\widehat{Hf}^{\circ}$ = heat of formation of reactants

ΔH_{vap}: Heat of vaporisation

n: number of mols

Q_{cal}: Heat transported

RMM = molecular weight of reactants

T1 = reference temperature (25 ºC)

T2 = temperature of the reactants

T_{evap} = evaporation temperature of the substance

Conflicts of Interest

The authors declare no conflicts of interest.

References

Amado Alviz, P.L., Alvarez, A.J., 2017. Comparative life cycle assessment of the use of an ionic liquid ([Bmim]Br) versus a volatile organic solvent in the production of acetylsalicylic acid.

J. Clean. Prod. 168, 1614–1624. https://doi.org/10.1016/j.jclepro.2017.02.107

Barros, S., Zwolinski, P., Mansur, A.I., 2017. Where do the environmental impacts of Additive Manufacturing come from? Case study of the use of 3d-printing to print orthotic insoles, in: 12ème Congrès International de Génie Industriel (CIGI 2017). Compiegne, p. 9.

Bekker, A.C.M., Verlinden, J.C., 2018. Life cycle assessment of wire + arc additive manufacturing compared to green sand casting and CNC milling in stainless steel. J. Clean. Prod. 177, 438–447. https://doi.org/10.1016/j.jclepro.2017.12.148

Blanchard, A.A., Phelan, J.W., Davis, A.R., 1936. Synthetic Inorganic Chemistry, 5th ed. John Wiley & Sons, Inc., London.

Booth, H.S., 1939. Inorganic Syntheses, Volume I., in: Booth, H.S. (Ed.), Inorganic Syntheses, Volume I Edited. McGraw-Hill Book Company, Inc., New York, pp. 151–157. https://doi.org/10.1002/9780470132326

Cerdas, F., Juraschek, M., Thiede, S., Herrmann, C., 2017. Life Cycle Assessment of 3D Printed Products in a Distributed Manufacturing System. J. Ind. Ecol. 21, S80–S93. https://doi.org/10.1111/jiec.12618

Cuéllar-Franca, R.M., García-Gutiérrez, P., Taylor, S.F.R., Hardacre, C., Azapagic, A., 2016. A novel methodology for assessing the environmental sustainability of ionic liquids used for CO2 capture. Faraday Discuss. 192, 283–301. https://doi.org/10.1039/C6FD00054A

de Bruijn, H., Duin, R. van, Huijbregts, M.A.J., 2002. Handbook on Life Cycle Assessment, Operational Guide to the ISO Standards. Kluwer Academic Publishers, USA. https://doi.org/10.1007/0-306-48055-7

DETHERM (Society for Chemical Engineering and Biotechnology), 2018. Thermophysical Property Data [WWW Document]. URL http://detherm.cds.rsc.org/detherm/index.php (accessed 5.11.18).

Ding, J., Shen, J., 2012. Method for preparation of N-vinylimidazole. Chinese Patent CN102382059 (A).

Ebel, K., Koehler, H., Gamer, A.O., Jäckh, R., 2002. Imidazole and Derivatives, in: Ullmann's Encyclopedia of Industrial Chemistry. Wiley-VCH Verlag GmbH & Co. KGaA, Weinheim. https://doi.org/10.1002/14356007

Energy UK, 2017. Energy in the UK. London.

Farahipour, R., Karunanithi, A., 2014. Life Cycle Environmental Implications of CO2 Capture and Sequestration with Ionic Liquid 1-butyl-3-methylimidazolium acetate. ACS Sustain. Chem.

Eng. 2, 2495–2500. https://doi.org/10.1021/sc400274b

Felder, R.M., Rousseau, R.W., 2005. Elementary Principes of Chemical Processes, 3rd ed. John Wiley & Sons, Inc., USA.

Frischknecht, R., Jungbluth, N., Althaus, H.-J., Doka, G., Dones, R., Heck, T., Hellweg, S., Hischier, R., Nemecek, T., Rebitzer, G., Spielmann, M., 2005. The ecoinvent Database: Overview and Methodological Framework (7 pp). Int. J. Life Cycle Assess. 10, 3–9. https://doi.org/10.1065/lca2004.10.181.1

Gebler, M., Schoot Uiterkamp, A.J.M., Visser, C., 2014. A global sustainability perspective on 3D printing technologies. Energy Policy 74, 158–167. https://doi.org/10.1016/J.ENPOL.2014.08.033

Gunasekera, D.H.A.T., Kuek, S., Hasanaj, D., He, Y., Tuck, C., Croft, A.K., Wildman, R.D., 2016. Three dimensional ink-jet printing of biomaterials using ionic liquids and co-solvents. Faraday Discuss. 190, 509–523. https://doi.org/10.1039/C5FD00219B

Gutowski, T., Jiang, S., Cooper, D., Corman, G., Hausman, M., Manson, J.-A., Schudeleit, T., Wegener, K., Sabelle, M., Ramos-Grez, J., Sekulic, D.P., 2017. Note on the Rate and Energy Efficiency Limits for Additive Manufacturing. J. Ind. Ecol. 21, S69. https://doi.org/10.1111/jiec.12664

Hischier, R., Hellweg, S., Capello, C., Primas, A., 2005. Establishing life cycle inventories of chemicals based on differing data availability. Int. J. Life Cycle Assess. 10, 59–67. https://doi.org/10.1065/lca2004.10.181.7

Huang, S.H., Liu, P., Mokasdar, A., Hou, L., 2013. Additive manufacturing and its societal impact: A literature review. Int. J. Adv. Manuf. Technol. 67, 1191–1203. https://doi.org/10.1007/s00170-012-4558-5

Huebschmann, S., Kralisch, D., Loewe, H., Breuch, D., Petersen, J.H., Dietrich, T., Scholz, R., 2011. Decision support towards agile eco-design of microreaction processes by accompanying (simplified) life cycle assessment. Green Chem. 13, 1694. https://doi.org/10.1039/c1gc15054e

ISO (The International Standards Organisation), 2006a. ISO 14040:2006 - Environmental management - Life Cycle Assessment - Principles and Framework. Int. Organ. Stand. 20.

ISO (The International Standards Organisation), 2006b. ISO 14044:2006 - Environmental management - Life cycle assessment - Requirements and guidelines. Int. Organ. Stand. 46.

Jacquemin, L., Pontalier, P.-Y., Sablayrolles, C., 2012. Life cycle assessment (LCA) applied to

the process industry: a review. Int. J. Life Cycle Assess. 17, 1028–1041. https://doi.org/10.1007/s11367-012-0432-9

Kamm, O., Marvel, C.S., 1921. Alkyl and Alkylene Bromides. Org. Synth. 1, 3. https://doi.org/10.15227/orgsyn.001.0003

Karjalainen, E., Aseyev, V., Tenhu, H., 2014. Influence of Hydrophobic Anion on Solution Properties of PDMAEMA. Macromolecules 47, 2103–2111. https://doi.org/10.1021/ma5000706

Karjalainen, E., Wales, D.J., Gunasekera, D.H.A.T., Dupont, J., Licence, P., Wildman, R.D., Sans, V., 2018. Tunable Ionic Control of Polymeric Films for Inkjet Based 3D Printing. ACS Sustain. Chem. Eng. 6, 3984–3991. https://doi.org/10.1021/acssuschemeng.7b04279

Kellens, K., Baumers, M., Gutowski, T.G., Flanagan, W., Lifset, R., Duflou, J.R., 2017. Environmental Dimensions of Additive Manufacturing: Mapping Application Domains and Their Environmental Implications. J. Ind. Ecol. 21, S49–S68. https://doi.org/10.1111/jiec.12629

Kralisch, D., Reinhardt, D., Kreisel, G., 2007. Implementing objectives of sustainability into ionic liquids research and development. Green Chem. 9, 1308. https://doi.org/10.1039/b708721g

Kralisch, D., Stark, A., Koersten, S., Kreisel, G., Ondruschka, B., 2005. Energetic, environmental and economic balances: Spice up your ionic liquid research efficiency. Green Chem. 7, 301–309. https://doi.org/10.1039/b417167e

Kreiger, M., Pearce, J.M., 2013. Environmental life cycle analysis of distributed three-dimensional printing and conventional manufacturing of polymer products. ACS Sustain. Chem. Eng. 1, 1511–1519. https://doi.org/10.1021/sc400093k

Li, Y., Linke, B.S., Voet, H., Falk, B., Schmitt, R., Lam, M., 2017. Cost, sustainability and surface roughness quality – A comprehensive analysis of products made with personal 3D printers. CIRP J. Manuf. Sci. Technol. 16, 1–11. https://doi.org/10.1016/j.cirpj.2016.10.001

Ma, J., Harstvedt, J.D., Dunaway, D., Bian, L., Jaradat, R., 2018a. An Exploratory Investigation of Additively Manufactured Product Life Cycle Sustainability Assessment. J. Clean. Prod. 192, 55–70. https://doi.org/10.1016/j.jclepro.2018.04.249

Ma, J., Harstvedt, J.D., Dunaway, D., Bian, L., Jaradat, R., 2018b. An Exploratory Investigation of Additively Manufactured Product Life Cycle Sustainability Assessment. J. Clean. Prod. 192, 55–70. https://doi.org/10.1016/j.jclepro.2018.04.249

Mecerreyes, D., 2011. Polymeric ionic liquids: Broadening the properties and applications of

polyelectrolytes. Prog. Polym. Sci. 36, 1629–1648. https://doi.org/10.1016/j.progpolymsci.2011.05.007

Mehrkesh, A., Karunanithi, A.T., 2016. Life-Cycle Perspectives on Aquatic Ecotoxicity of Common Ionic Liquids. Environ. Sci. Technol. 50, 6814–6821. https://doi.org/10.1021/acs.est.5b04721

Mehrkesh, A., Karunanithi, A.T., 2013. Energetic ionic materials: How green are they? A comparative life cycle assessment study. ACS Sustain. Chem. Eng. 1, 448–455. https://doi.org/10.1021/sc3001383

NIST (National Institute of Standards and Technology), 2018. NIST Chemistry WebBook [WWW Document]. NIST Chem. Webb. URL https://webbook.nist.gov/chemistry/ (accessed 5.11.18).

OECD, 2017. 3D printing and its environmental applications, in: The Next Production Revolution: Implications for Governments and Business. OECD, Paris, pp. 171–213. https://doi.org/10.1787/9789264271036-en

Peng, T., 2016. Analysis of Energy Utilization in 3D Printing Processes. Procedia CIRP 40, 62–67. https://doi.org/10.1016/j.procir.2016.01.055

Peterson, J.E., 2013. Ionic Liquid/CO2 Co-Fluid Refrigeration: CO2 Solubility Modeling and Life Cycle Analysis. PhD Thesis, University of Notre Dame.

PRé Consultants, 2014. SimaPro Database Manual - Methods Library. San Francisco.

Qian, W., Texter, J., Yan, F., 2017. Frontiers in poly(ionic liquid)s: syntheses and applications. Chem. Soc. Rev. 46, 1124–1159. https://doi.org/10.1039/C6CS00620E

Quinlan, H.E., Hasan, T., Jaddou, J., Hart, A.J., 2017. Industrial and Consumer Uses of Additive Manufacturing: A Discussion of Capabilities, Trajectories, and Challenges. J. Ind. Ecol. 21, S15–S20. https://doi.org/10.1111/jiec.12609

Righi, S., Morfino, A., Galletti, P., Samorì, C., Tugnoli, A., Stramigioli, C., 2011. Comparative cradle-to-gate life cycle assessments of cellulose dissolution with 1-butyl-3-methylimidazolium chloride and N-methyl-morpholine-N-oxide. Green Chem. 13, 367. https://doi.org/10.1039/c0gc00647e

Sans, V., Karbass, N., Burguete, M.I., Compañ, V., García-Verdugo, E., Luis, S. V., Pawlak, M., 2011. Polymer-Supported Ionic-Liquid-Like Phases (SILLPs): Transferring Ionic Liquid Properties to Polymeric Matrices. Chem. - A Eur. J. 17, 1894–1906. https://doi.org/10.1002/chem.201001873

Schultz, A.R., Lambert, P.M., Chartrain, N.A., Ruohoniemi, D.M., Zhang, Z., Jangu, C., Zhang, M., Williams, C.B., Long, T.E., 2014. 3D printing phosphonium ionic liquid networks with mask projection microstereolithography. ACS Macro Lett. 3, 1205–1209. https://doi.org/10.1021/mz5006316

Shaplov, A.S., Ponkratov, D.O., Vygodskii, Y.S., 2016. Poly(ionic liquid)s: Synthesis, properties, and application. Polym. Sci. Ser. B 58, 73–142. https://doi.org/10.1134/S156009041602007X

Stouffer, S., Guttman, L., Suchman, E., Lazarsfeld, P.F., Star, S., Clausen, J., 2008. Heat Capacities of Ionic Liquids as a Function of Temperature at 0.1 MPa. Measurement and prediction. J. Chem. Eng. Data 53, 2148–2153. https://doi.org/10.1021/je800335v

Vatani, A., Mehrpooya, M., Gharagheizi, F., 2007. Prediction of standard enthalpy of formation by a QSPR model. Int. J. Mol. Sci. 8, 407–432. https://doi.org/10.3390/i8050407

Wales, D.J., Cao, Q., Kastner, K., Karjalainen, E., Newton, G.N., Sans, V., 2018. 3D-Printable Photochromic Molecular Materials for Reversible Information Storage. Adv. Mater. 30, 1800159. https://doi.org/10.1002/adma.201800159

Welton, T., 1999. Room-Temperature Ionic Liquids. Solvents for Synthesis and Catalysis. Chem. Rev. 99, 2071–2083. https://doi.org/10.1021/cr1003248

Yanchun Luo, Zhiming Ji, Leu, M.C., Caudill, R., 1999. Environmental performance analysis of solid freedom fabrication processes. Proc. 1999 IEEE Int. Symp. Electron. Environ. (Cat. No.99CH36357) 1–6. https://doi.org/10.1109/ISEE.1999.765837

Yang, Y., Li, L., Pan, Y., Sun, Z., 2017. Energy Consumption Modeling of Stereolithography-Based Additive Manufacturing Toward Environmental Sustainability. J. Ind. Ecol. 21, S168–S178. https://doi.org/10.1111/jiec.12589

Yu, H., Zhang, C., Anderson, J.L., 2015. Ionic Liquids and Polymeric Ionic Liquids in Analytical Environmental Applications, in: Mecerreyes, D. (Ed.), Applications of Ionic Liquids in Polymer Science and Technology. Springer Berlin Heidelberg, Berlin, pp. 153–198. https://doi.org/10.1007/978-3-662-44903-5_7

Yuan, J., Mecerreyes, D., Antonietti, M., 2013. Poly(ionic liquid)s: An update. Prog. Polym. Sci. 38, 1009–1036. https://doi.org/10.1016/j.progpolymsci.2013.04.002

Zhang, Y., Bakshi, B.R., Demessie, E.S., 2008. Life cycle assessment of an ionic liquid versus molecular solvents and their applications. Environ. Sci. Technol. 42, 1724–1730. https://doi.org/10.1021/es0713983